Progression rate of backward erosion piping in laboratory experiments and reliability analysis

Pol, Joost; van Beek, Vera; Kanning, Wim; Jonkman, Sebastiaan N.

DOI
10.3850/978-981-11-2725-0_IS4-3-cd

Publication date
2019

Document Version
Final published version

Published in
7th International Symposium on Geotechnical Safety and Risk (ISGSR 2019)

Progression Rate of Backward Erosion Piping in Laboratory Experiments and Reliability Analysis

J.C. Pol[1], V.M. van Beek[2], W. Kanning[3], and S.N. Jonkman[4]

[1]Delft University of Technology, Stevinweg 1 Delft, The Netherlands. E-mail: J.C.Pol@tudelft.nl
[2]Deltares, Boussinesqweg 1 Delft, The Netherlands. E-mail: Vera.vanBeek@deltares.nl
[3]Delft University of Technology, Stevinweg 1 Delft, The Netherlands. E-mail: W.Kanning@tudelft.nl
[4]Delft University of Technology, Stevinweg 1 Delft, The Netherlands. E-mail: S.N.Jonkman@tudelft.nl

Abstract: Backward erosion piping is an important failure mode of dikes and dams. The time required for the backward erosion process to result in dike failure is expected to be an important factor in the safety of dikes. This holds especially in coastal and estuarine areas which are dominated by storm surge, and pipes may not fully develop during a storm. Furthermore, insight in the duration of the various piping stages can assist in developing effective emergency mitigation measures. However, the temporal development of piping is hardly studied quantitatively, as most experimental and modelling studies focus on the critical head. Also data of real breaches is generally insufficient to determine the time to failure. As a result, currently the contribution of time required for pipe growth cannot be quantified in a deterministic and reliability analysis. In this study, it is investigated how the pipe progression rate can be predicted and applied to dike reliability. The data analysis is based on a composition of 45 small, medium and large scale experiments from six studies. Advancement rates are related to the applied hydraulic gradient and soil properties using a multivariate analysis. From the analysis we derive an empirical model for the advancement rate, including a quantification of the uncertainty. This model is applied in a reliability analysis of a hypothetical coastal and riverine dike. The results of our analysis may be used to validate transient numerical piping models, perform time-dependent probabilistic dike safety analysis and support emergency response.

Keywords: Piping; dikes; temporal development; progression rate; experiments; reliability.

1 Introduction

Failure of dikes may occur due to a range of failure modes such as overflow, slope instability or internal erosion. This study focusses on the mechanism of backward erosion piping (in short piping) which is a form of internal erosion. A factor that receives relatively little attention in the literature is the temporal development of the piping process. This temporal development depends on three main factors: (1) the development of the hydraulic load, (2) the response of aquifer pressures to this load and (3) pipe growth. Pipe growth can be broken down into (3a) a regressive phase when the pipe can reach an equilibrium, (3b) a progressive phase after the equilibrium is lost and (3c) the widening phase. Conventional piping assessments usually model the critical load (head difference or hydraulic gradient) in a steady state condition, e.g. the model of Sellmeijer et al. (2011). These models assume steady state groundwater flow and instantaneous pipe progression. However, if the pipe develops relatively slowly compared to flood duration, water levels may recede before the pipe has fully developed and no failure occurs during a flood. Historical failures show that the development of piping may take a few hours - e.g. in New Orleans during Hurricane Katrina (USACE 2007) - to several days (Tu 2014).

The central question with respect to the temporal development of piping investigated in this paper is how to predict the piping progression rate during the progressive phase, and how to apply this information in a dike reliability analysis. The significance of the factor time is expected to depend strongly on both dike geometry and subsoil characteristics, the hydraulic loads and the uncertainties present in these parameters. Most piping research has focused on understanding the physical processes of e.g. groundwater flow, soil stability and soil erosion without integrating it in a reliability framework or combining it with knowledge on flood duration. This raises the question to what extent time-dependence is significant for the entire dike safety, and in which situations a positive contribution can be expected.

2 Methods

The approach in this paper consists of two parts: (1) an analysis of progression rates in existing experiments and (2) an application of these findings in a reliability analysis of a hypothetical dike.

2.1 Experimental data

Experimental data is composed of 45 tests from six test series with different setups. Table 1 summarizes the dataset including ranges of seepage length L, grain size d_{70}, porosity n, hydraulic conductivity k. Figure 1a shows a cross section of a common setup. The head is increased stepwise until no equilibrium is reached anymore

Proceedings of the 7th International Symposium on Geotechnical Safety and Risk (ISGSR)
Editors: Jianye Ching, Dian-Qing Li and Jie Zhang

Published by Research Publishing, Singapore.
ISBN: 978-981-11-2725-0; doi:10.3850/978-981-11-2725-0_IS4-3-cd

(Figure 1b). This head is defined as the critical head H_c. The pipe length at that moment is the critical length l_c. The pipe progression rate v [L/T] (or pipe growth velocity or advancement rate) is defined as the increase in straight pipe length l [L] over a given period of time t [T]. In this analysis we use the average rate over the period between the time at which the critical length is reached and at which the pipe length is equal to the seepage length L: $v_{c,avg} = (L-l_c)/(t_{end}-t_c)$.

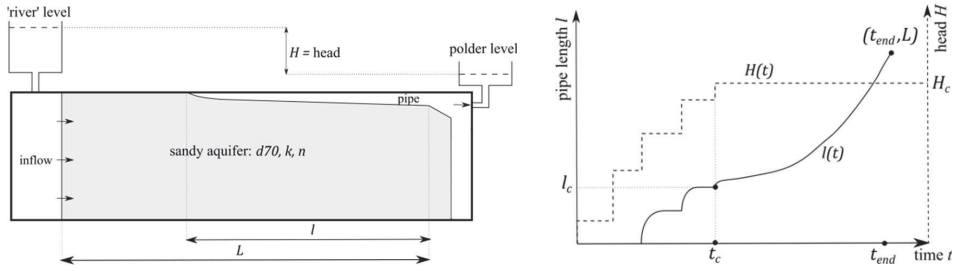

(a) Experimental setup (slope type box). **(b)** Typical development of head and pipe length

Figure 1. Definitions in progression rate analysis.

A number of experiments have been reviewed. The tests by Van Beek et al. (2012) are small- and medium scale tests in rectangular boxes with a slope type exit, and several sand types were used. Yao's tests include a two-layer stratum (fine on coarse) in small scale boxes with slope and hole type exits. The fine sand properties are used in this analysis. The three full scale IJkdijk tests (Sellmeijer et al. 2011) are performed on a newly constructed clay dike on fine and coarse sands, and have a plane type exit. Robbins et al. (2017) use cylinders instead of boxes. In these tests, the critical head is not always kept constant during progression. Vandenboer et al. (2018) used a box with hole exit, and applied sudden supercritical heads instead of a stepwise increasing head. Progression rates vary between $5 \cdot 10^{-5}$ and $2 \cdot 10^{-3}$ m/s (4-170 m/day).

Table 1. Piping experiments analyzed in this paper.

Source	Nr. of tests	Setup	L (m)	d_{70} (m)	n (-)	k (m/s)	H_c (m)
Van Beek et al. (2012) SS	12	box, slope	0.3	$1.5\text{-}4.3 \cdot 10^{-4}$	0.34-0.40	$0.5\text{-}10 \cdot 10^{-4}$	0.07-0.18
Van Beek et al. (2012) MS	7	box, slope	1.3-1.45	$1.5\text{-}2.1 \cdot 10^{-4}$	0.38-0.40	$1.7\text{-}3.7 \cdot 10^{-4}$	0.19-0.37
Yao (2014)	7	box, hole/slope, multilayer	0.35	$1.5 \cdot 10^{-4}$	0.35-0.36	$0.56 \cdot 10^{-4}$	0.06-0.13
Sellmeijer et al. (2011)	3	plane type	15	$1.8\text{-}2.6 \cdot 10^{-4}$	0.37-0.40	$0.8\text{-}1.4 \cdot 10^{-4}$	1.75-2.3
Robbins et al. (2017)	14	cylinder, slope	0.95	$3.3 \cdot 10^{-4}$	0.38-0.42	$4.8\text{-}12 \cdot 10^{-4}$	0.2-0.4
Vandenboer et al. (2018)	2	box, hole	0.3	$1.9 \cdot 10^{-4}$	0.40	$1.0 \cdot 10^{-4}$	0.06-0.08

2.2 Prediction of progression rate

To identify important factors that predict the progression rates, correlations between the average progression rate in an experiment and the parameters in Table 1 were established; visually using scatterplots and quantitatively using the (Kendall) rank correlation coefficient. A multivariate linear regression model (Eq. 1) was created by stepwise addition of variables in Table 1. First, the variables $v_{c,avg}$, k and d_{70} were made dimensionless by scaling with their mean values: $\bar{v}_{c,avg} = 6.5 \cdot 10^{-4}$ m/s, $\bar{k} = 3.4 \cdot 10^{-4}$ m/s, $\bar{d}_{70} = 2.4 \cdot 10^{-4}$ m. After that, a logarithmic transformation of v, H_c/L and k was applied because the scatterplots indicated a logarithmic relation:

$$\log\left(\frac{v_{c,avg}}{\bar{v}_{c,avg}}\right) = a_1 + a_2 \cdot \log\left(\frac{H_c}{L}\right) + a_3 \cdot \log\left(\frac{k}{\bar{k}}\right) + a_4 \cdot \frac{d_{70}}{\bar{d}_{70}} + a_5 \cdot n \tag{1}$$

In addition to this purely statistical model, another model was applied to the data that is based on the assumption of proportionality between the progression rate and the pore velocities at the pipe tip (Kezdi 1979):

$$v_c(t) = \frac{dl}{dt} = \frac{c \cdot k \cdot H(t)}{\left(L - l(t)\right) \cdot n} \tag{2}$$

In which c is the proportionality constant. Note that this model assumes a linear decrease in head between upstream level and pipe tip and no head drop in the pipe, although the actual head drop is nonlinear due to flow concentration and there will also be a pipe head drop. By solving the differential equation in Eq. (2) for a constant head $H(t)=H_c$, it can be shown that this model leads to the following average progression rate:

$$v_{c,avg} = \frac{2 \cdot c \cdot k \cdot H_c}{L \cdot n} \tag{3}$$

2.3 Reliability analysis

Monte Carlo analysis is used to for the reliability modeling of the time-dependent processes. Failure is defined by the limit state function (LSF) in Eq. (4), which describes that failure occurs if the pipe length l equals the present seepage length L, i.e. when there is a hydraulic shortcut between river and polder side. The LSF is evaluated each time step during a flood wave.

$$Z_b(t) = L - l(t) \tag{4}$$

The temporal development of l is described by a pipe progression model (section 2.3.1). The seepage length L in the LSF and variables in the progression model are sampled randomly from their distributions (Table 2) at t=0, and realizations are kept equal in different time steps. Only the water level (modeled with random variables peak level h_{max} and duration T) and pipe length are time-dependent. Therefore, each realization results in a time series of the limit state and failure occurs when $Z_b(t)$ becomes lower than 0 during the modeled flood wave.

A number of simplifications are made in this analysis. First, there is no damping or delay in the aquifer head response to the water level. This is considered a reasonable assumption for confined sandy aquifers with an impervious blanket. Secondly, we assume that the widening and collapse process occurs instantaneously when the pipe connects to the upstream side. Random variables are assumed to be uncorrelated.

2.3.1 Modeling piping progression l(t)

Pipe progression as function of the random variables and time is calculated using Eq. (2) and a set of three conditions that must be met before pipe progression can occur. Following TAW (1999), these conditions are (a) uplift and rupture of the cohesive cover, (b) heave or vertical transport of grains and (c) loss of grain stability in the horizontal pipe. The condition for uplift ($Z_u(t)$) is based on the difference between upward pressure at the inner toe and the weight of the cover layer. This depends on the river head $h(t)$ and polder head h_p and the thickness (d) and weight ($\gamma_{c,sat}$) of the cover layer (TAW 1999):

$$Z_u(t) = H(t) - H_{c,u} = (h(t) - h_p) - d \cdot (\gamma_{c,sat} - \gamma_{water}) / \gamma_{water} \tag{5}$$

The condition for heave ($Z_h(t)$) is based on the critical heave gradient at the inner toe $i_{c,h}$ (TAW, 1999), which is the hydraulic gradient needed to transport particles vertically through the crack in the cover layer:

$$Z_h(t) = i(t) - i_{c,h} = (h(t) - h_p) / d - i_{c,h} \tag{6}$$

The condition for (steady-state) pipe grain stability ($Z_s(t)$) is given by Eq. (7), in which the critical head that is needed to enter the progressive ($H_{c,p}$) is calculated using the revised Sellmeijer rule (Sellmeijer et al. 2011):

$$Z_s(t) = h(t) - H_{c,p} = h(t) - h_p - L \cdot F_R \cdot F_s \cdot F_G \tag{7}$$

The resistance factor F_R depends on θ (bedding angle), η (White's coefficient) and the particle diameter d_{70}, the shape factor F_S on d_{70} and L, and the geometry factor F_G on the D/L ratio.

When the critical head for progression is reached ($h=H_{c,p}$; $Z_s=0$), we assume that the pipe length equals the critical pipe length ($l=l_c$) and the progressive phase (subject of this paper and eqn. (2)) is entered for $l>l_c$. Actually, l_c depends on the geometry of the aquifer, but is assumed to be ½L (Sellmeijer and Koenders 1991). From that moment ($l>l_c$), the pipe progression rate $v_c(t)$ as given by Eq. (2) can be used to calculate the pipe progression dl/dt if uplift occurred earlier in the flood wave and heave still occurs. Otherwise dl/dt=0:

$$\frac{dl}{dt}(t) = \begin{cases} v_c(t) & \text{if } (\min\{Z_u\} < 0) \cap (Z_h(t) < 0) \cap (\min\{Z_s\} < 0) \\ 0 & \text{else} \end{cases} \tag{8}$$

Hence, $l(t)$ is calculated on every time step Δt for the flood wave duration T by using Eq. (8):

$$l(t) = l(t-\Delta t) + \frac{dl}{dt}\cdot\Delta t \tag{9}$$

This starts at the moment $Z_s < 0$ and thus $l=l_c$ for the considered progression phase.

2.3.2 Variables for dike case study

Five cases were defined, based on flood type/duration (riverine or coastal) and seepage length (50 or 100 m). All other random and deterministic variables are the same in the five cases and are given in Figure 2 and Table 2. The riverine flood wave is modeled as trapezium with peak duration T_{max} and base duration T_{base}. The coastal flood wave is a trapezoidal storm setup added to the tidal amplitude of 2 m.

Table 2. Distributions of random variables used in Monte Carlo analysis.

Stochastic (equal in cases)		**Case specific**			**Deterministic**	
L (m)	see Table 3		<u>*Riverine*</u>	<u>*Coastal*</u>		
D (m)	N(25,5)	h_{max} (m+NAP)	Gum(1.5,0.5)	Gum(3,0.5)	θ (°)	37
d (m)	N(2,0.2)	T_{max} (h)	12	2	η (-)	0.25
$\gamma_{c,sat}$ (kN/m^3)	N(16,1.6)	T_{base} (h)	480	48	l_c/L (-)	0.5
d_{70} (10^{-4} m)	N(3.5,0.5)	h_p (m+NAP)	0	2	γ_{water} (kN/m^3)	10
n (-)	N(0.35, 0.01)	h_{base} (m+NAP)	1	2		
k (10^{-4} m/s)	N(4,2)					
$i_{c,h}$	N(0.5, 0.1)					
m_v (-)	Logn(0,0.7)					

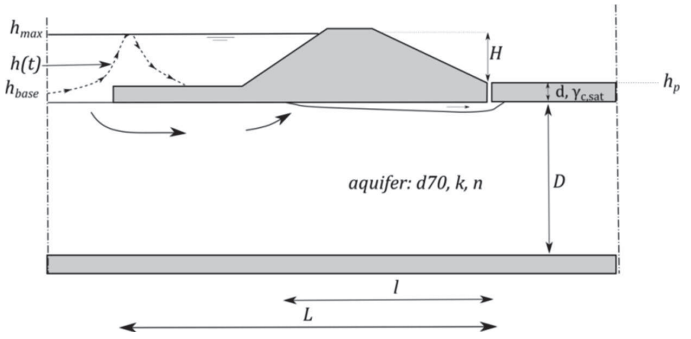

Figure 2. Dike schematization for reliability analysis.

3 Results

3.1 Progression rate analysis

The critical gradient, the hydraulic conductivity and the grain size have a significant correlation with the progression rate (Kendall's τ = 0.25-0.39). No relation between progression rate and porosity or relative density was found. This can be explained by the fact that the variation in porosity is relatively small compared to the other variables, and secondly because it is correlated with the conductivity. The grain size is also strongly correlated to hydraulic conductivity and therefore does not improve the prediction. Therefore, H_c/L and k are used as predictors in the statistical model. Omitting d_{70} and n from Eq. (1) yields:

$$v_{c,avg} = \bar{v}_{c,avg}\cdot 10^{a_1}\cdot\left(\frac{Hc}{L}\right)^{a_2}\cdot\left(\frac{k}{\bar{k}}\right)^{a_3} \tag{10}$$

The best fit for Eq. (10) is found for coefficients a_1=0.79, a_2=1.4, a_3=0.57. The best fit of Eq. (2) is found for c=1.6. This results in a R^2 value of 0.66 and 0.40 respectively (see Figure 3). Figure 3 shows that the order of magnitude is predicted well for a wide range of experimental setups. The lower panels show the model uncertainty ($m_v=v_{exp}/v_{model}$) including a fit of a lognormal density function.

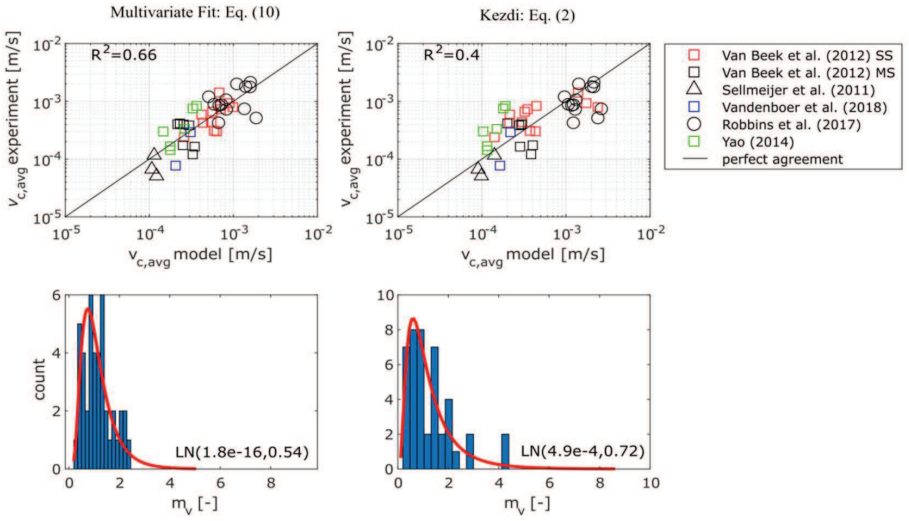

Figure 3. Correspondence between experimental data and predictions of Eq. (2) and Eq. (10).

3.2 Dike reliability case study

The reliability analysis shows how the pipe progression rate contributes to dike safety in five hypothetical scenarios. Figure 4 illustrates the (normalized) Z-values (dashed lines) together with the water level time series for one Monte Carlo realization of the coastal case. It can be seen that in this case the critical head is reached just before the flood peak (Z_S <0, at t=-2 hours). From that moment, the pipe grows from l_c towards L during high water, resulting in a decreasing Z_B-value (purple line). During low tide (t=4-11 hours) the pipe growth pauses as the head is too low for heave (Z_H >0). Although there is further pipe growth during the next high tide, the storm is too short to complete the pipe progression. Therefore no failure occurs in this realization: $Z_B(t=40)>0$.

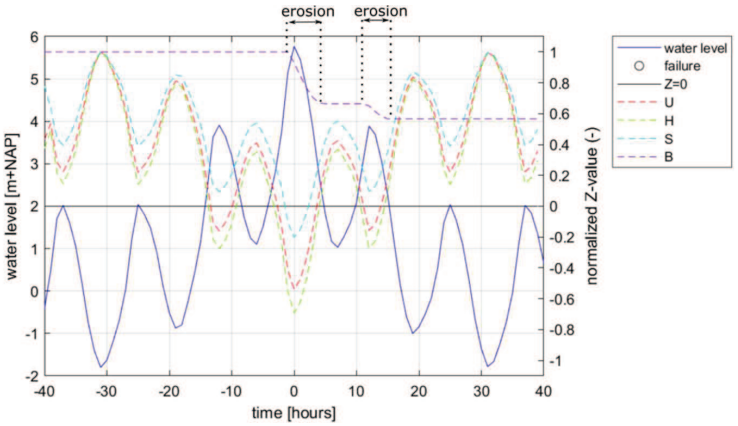

Figure 4. Development of Z-values during the flood wave. Example for one realization of coastal case 3 (mean seepage length 50 m, peak duration 2 h, base duration 48 h). U=uplift, H=heave, S=critical head for progression, B=pipe growth.

Table 3 shows the resulting failure probabilities P_f of the five cases, using both Eq. (2) and Eq. (10). $P_{f,stat}$ is for stationary computation (instantaneous pipe growth), $P_{f,td}$ is including pipe progression rates. $F_{TD}= P_{f,stat}/P_{f,td}$ indicates the effect on dike safety. In the riverine cases, the failure probability decreases with a factor 1-2. In the coastal cases the effect is much larger due to the shorter flood duration; a factor 3-30 decrease with Eq. (2) up to a factor 53-10^4 with Eq. (10). The latter gives larger effects, because for these full scale dike configurations, Eq. (10) gives a factor 10 lower progression rates than Eq. (2). It must be noted that the increase in reliability is only due to the time required for pipe progression. In reality, there may also be a contribution from the delay and damping of the groundwater response, the widening process, and emergency measures. For realizations that still fail in the time-dependent computation, the average delay τ in the moment of failure caused by the pipe

progression rates is calculated. $\mu(\tau)$ in Table 3 indicates the average delay, $\mu(v)$ indicates the erosion rate averaged over the realizations.

Table 3. Summary of reliability analysis results for several cases.

Case	Flood duration	L (m)	$P_{f,stat}$ (1/yr)	Kézdi: Eq. (2) $P_{f,td}$ (1/yr)	Kézdi: Eq. (2) F_{TD} (-)	Kézdi: Eq. (2) $\mu(\tau)$ (h)	Kézdi: Eq. (2) $\mu(v)$ (m/s)	Multivariate Fit: Eq. (10) $P_{f,td}$ (1/yr)	Multivariate Fit: Eq. (10) F_{TD} (-)	Multivariate Fit: Eq. (10) $\mu(\tau)$ (h)	Multivariate Fit: Eq. (10) $\mu(v)$ (m/s)
1	riverine	$N(50,5)$	$5.0\cdot10^{-2}$	$5.0\cdot10^{-2}$	1	17	$8.5\cdot10^{-4}$	$4.9\cdot10^{-2}$	1.05	70	$12\cdot10^{-5}$
2	riverine	$N(100,5)$	$5.2\cdot10^{-4}$	$5.1\cdot10^{-4}$	1	37	$7.8\cdot10^{-4}$	$2.6\cdot10^{-4}$	2	119	$8.3\cdot10^{-5}$
3	coastal	$N(50,5)$	$1.9\cdot10^{-2}$	$2.0\cdot10^{-3}$	9	8	$5\cdot10^{-4}$	$2\cdot10^{-6}$	10^4	25	$7.7\cdot10^{-5}$
4	coastal	$N(25,5)$	$2.1\cdot10^{-1}$	$7.0\cdot10^{-2}$	3	6	$7\cdot10^{-4}$	$3.6\cdot10^{-3}$	53	17	$14\cdot10^{-5}$
5	coastal	$N(75,5)$	$2.0\cdot10^{-3}$	$7\cdot10^{-5}$	30	7	$3.5\cdot10^{-4}$	$<10^{-6}$	$>10^3$	-	$5.8\cdot10^{-5}$

4 Conclusions

This paper analyses the average pipe progression rates in 45 backward erosion piping experiments from six datasets. A large variety of test configurations is covered, creating a larger range in outcomes as the erosion process is affected by the type of setup. The progression rates vary from $5\cdot10^{-5}$ to $2\cdot10^{-3}$ m/s, and can be predicted reasonably well by the (critical) hydraulic gradient and the hydraulic conductivity. As can be expected because of scale effects, the lowest values are found in the full scale tests. Therefore, the lower values are expected to be more representative for field conditions. Due to the considerable uncertainty in the predictive formulas, care should be taken in the application of these to situations outside the range of the experiments.

Secondly, it is shown how these progression rates can be included in a reliability analysis of backward erosion in dikes. For this purpose a Monte Carlo framework was adopted/developed that includes multiple time-dependent limit state functions. Application of this framework to five hypothetical cases shows the possible contribution to dike safety of the inclusion of the pipe growth process. The chosen flood durations are two extremes for water systems in the Netherlands: a relatively long riverine (Rhine) flood wave and a short coastal storm surge. Effects on the failure probability are small for the riverine cases (factor 1-2), but much larger for the coastal cases (factor 3-10^4). In the riverine area, there is still a significant delay in the expected time of failure of several days, which is beneficial for emergency response.

Future work should further explain the differences in the found progression rates, the underlying mechanism and scale effects. Subsequently, the reliability analysis should be extended and applied to more dike sections, to assess the potential of including these aspects in safety assessments and emergency strategies. More research is also needed into the effect of a partly developed pipe that is already present at the start of a flood event.

Acknowledgments

This work is part of the Perspectief research programme All-Risk with project number P15-21D, which is (partly) financed by NWO Domain Applied and Engineering Sciences.

References

Kézdi, R. (1979). *Soil Physics: Selected Topics,* Elsevier, Amsterdam, The Netherlands.

Robbins, B. A., Van Beek, V. M., Lopez-Soto, J. F., Montalvo-Bartolomei, A. M., and Murphy, J. (2017). A novel laboratory test for backward erosion piping. *International Journal of Physical Modelling in Geotechnics*, 18(5), 266-279.

Sellmeijer, J. B. and Koenders, M. A. (1991). A mathematical model for piping. *Applied Mathematical Modelling*, 15(11-12), 646-651.

Sellmeijer, H., de la Cruz, J. L., van Beek, V. M., and Knoeff, H. (2011). Fine-tuning of the backward erosion piping model through small-scale, medium-scale and ijkdijk experiments. *European Journal of Environmental and Civil Engineering*, 15(8), 1139-1154.

TAW (1999). *Technical Report on Sand Boils* (in Dutch), Rijkswaterstaat DWW, Delft, The Netherlands.

Tu, P. Q. (2014). *Reliability Analysis of the Red River Dikes System in Viet Nam*, Delft University of Technology, Delft, The Netherlands.

USACE (2007). *Performance Evaluation of the New Orleans and Southeast Louisiana Hurricane Protection System. Volume V – The Performance — Levees and Floodwalls*, USACE report.

Van Beek, V. M., Knoeff H., and Sellmeijer, J.B. (2011). Observations on the process of backward erosion piping in small-, medium- and full-scale experiments. *European Journal of Environmental and Civil Engineering*, 15(8), 1115-1137.

Vandenboer, K., Celette, F., and Bezuijen, A. (2018). The effect of sudden critical and supercritical hydraulic loads on backward erosion piping: Small-scale experiments. *Acta Geotechnica*, 1-12.

Yao, Q. (2014). *Multi-Size Experiments and Numerical Simulation for Backward Erosion Piping in Dike Foundations* (in Chinese). PhD Thesis, China Institute of Water Resources and Hydropower Research (IWHR), Beijing, China.